KFKI-71-34

G. Serfőző
P. Gróz

NMR STUDIES ON $KNiF_3$ AND $RbFeF_3$

Hungarian Academy of Sciences

CENTRAL
RESEARCH
INSTITUTE FOR
PHYSICS

BUDAPEST

KFKI-71-34

NMR STUDIES ON $KNiF_3$ and $RbFeF_3$

G. Serfőző
Department of Solid State Physics

P. Gróz
Department of Nuclear Chemistry
Central Research Institute for Physics, Budapest, Hungary

ABSTRACT

The NMR spectra of ^{19}F in polycrystalline samples of paramagnetic $KNiF_3$ and $RbFeF_3$ have been measured. The fractions of unpaired spins in the 2s- and 2p-orbitals of F^- were determined. The values of the isotropic f_{2s} and anisotropic $f_{\sigma-\pi}$ fractions of unpaired spins were found to be anomalously small in $RbFeF_3$.

РЕЗЮМЕ

Исследованы спектры ЯМР на ядрах фтора в поликристаллическом $KNiF_3$ и $RbFeF_3$. Определена спиновая плотность для 2s и 2p-оболочках фтора. Получено необычно малое значение спиновой плотности f_{2s} и $f_{\sigma-\pi}$ для $RbFeF_3$.

KIVONAT

Megvizsgáltuk $KNiF_3$ és $RbFeF_3$ polikristályos anyagmintáinak NMR spektrumát paramágneses állapotban. Meghatároztuk a paramágneses ionok delokalizált, nem kompenzált spinü elektronjainak a spinsürüségét a fluor mag helyén. Megállapitottük, hogy a $RbFeF_3$ esetében az f_s izotróp és $f_{\sigma-\pi}$ anizotróp spinsürüség értéke anomálisan kicsi.

INTRODUCTION

Electron delocalization

$KNiF_3$ and $RbFeF_3$ are materials of perovskite-type structure that are antiferromagnetic at low temperatures. This antiferromagnetism is due to super exchange interaction between unpaired 3d-electrons of the paramagnetic atoms. In these compounds the 4Å distance between neighbouring paramagnetic atoms does not permit direct overlapping of the 3d-electron orbitals, so the exchange effect is accomplished through molecular orbital complexes built up from the electron orbitals of a paramagnetic ion and the electron orbitals of the six surrounding fluorine atoms. Although the bonds which are formed are partially covalent in character, they differ from conventional covalent bonds in that the delocalization of the electrons is not limited to one complex, across the electron orbitals of the fluorine atoms can extend over several complexes [15].

This delocalization of unpaired 3d-electrons is studied in the following. The values of the nucleus-electron hyperfine interactions and the spin densities of the unpaired 3d-electrons in the different symmetry 2s- and 2p-orbitals of the fluorine atoms have been determined at the nuclear sites.

Spin density at the site of the fluorine nucleus

The percentage spin density of 3d-electrons with uncompensated spins /the fraction of unpaired spins/ in a given electron orbital can be defined by regarding the spin density of the orbital as 100% if it is found to contain only one spin-up electron. In reality spin densities as great as this are never found, since the 3d-electrons always admix with a small probability to the fluorine electron orbitals.

The spin density is determined in practice by comparing the theoretically calculated hyperfine field for the 100% spin density case with the experimental values, which are usually measured by NMR method. The theoretical values have been calculated by Moriya [11].

Only the partially filled "magnetic" orbitals at the E_g and T_{2g} symmetry levels are important with regard to the hyperfine field /see Fig. 2/. The spin density for each orbital must be determined separately.

Hyperfine field. I. Delocalized electrons

In MF_6-type complexes the 3d-electrons forming the σ-and π-bonds admix into the electron orbitals of the six fluorine atoms /Fig. 1/. The nucleus — electron hyperfine interaction differs from zero only for the unpaired electrons. In the hyperfine interaction of the delocalized electrons with the fluorine atoms the magnetic field at the fluorine nuclei in the z-direction is

$$H^{z}_{deloc} = - \frac{\langle s\rangle_{z,T}}{\gamma\hbar} \left[A_s + \sum_{\alpha=\sigma,\pi} A_\alpha (3 \cos^2\theta_{\alpha,z} - 1) \right] = Hs+Hp \qquad /1/$$

where $\langle s\rangle_{z,T}$ is the thermal average value of the electrons with unpaired spins, $\theta_{\alpha,z}$ is the angle between the internuclear radius and the external magnetic field, which is calculated separately for each σ-and π-bond /see Fig. 1/. A_s is the isotropic component of the hyperfine interaction arising from unpaired spins in the fluorine 2s-orbital, A_σ and A_π are the anisotropic components of the hyperfine interactions arising from unpaired electrons participating in the 2p-orbitals [3]. The directions are as shown in Fig. 1.

The values of the hyperfine interaction and the spin densities f_s, f_σ, and f_π are related by the following expressions

$$A_s = f_s \cdot a_{2s} \cdot (1/2s) \qquad /2/$$

$$A_\sigma - A_\pi = A_{\sigma-\pi} = f_{\sigma-\pi} \cdot a_{2p} \cdot (1/2s) = (f_\sigma - f_\pi)_{2p} \cdot a_{2p} \cdot (1/2s) \qquad /3/$$

The f_σ and f_π spin densities cannot be determined separately. a_{2s} and a_{2p} appear as constants in Moriya's theoretical calculations for 100% spin densitiy [11], and have the following values:

$$a_{2s} = (8\pi/3) \cdot g \cdot \mu_B \gamma_N \hbar \left|\psi_{2s}(0)\right|^2 = 1{,}503 \text{ cm}^{-1} \qquad /4/$$

$$a_{2p} = (2/5) \cdot g \cdot \mu_B \gamma_N \hbar \langle 1/r^3\rangle = 0{,}0429 \text{ cm}^{-1} \qquad /5/$$

The quantum number S for the paramagnetic ion in the high spin state is $S = 2$ for Fe^{2+} and $S = 1$ for Ni^{2+}. $|\psi_{2s}(o)|^2$ is the density of 2s-electrons at the fluorine nucleus, $\langle 1/r^3 \rangle$ is a mean value calculated for the fluorine 2p-orbital.

Hyperfine field. II. Localized electrons

Apart from the effect of the delocalized electrons, and of comparable size, there also arises a nuclear spin electron spin dipole-dipole interaction between the localized electron spin of the paramagnetic ion, with a thermal average value of $\langle s \rangle_{z,T}$, and the fluorine nucleus. The angular dependence of the contribution of this anisotropic hyperfine interaction is equal to that of the anisotropic hyperfine interaction of the delocalized electrons. This property makes it possible to separate the dipole contribution [10,18]. The latter can be expressed in the following form:

$$H_D^z = \sum_{k,i} \frac{\mu_B g \langle s \rangle_{z,T}}{r_{ik}^3} (3 \cos^2\Theta_{r_{ik}z} - 1) = \sum_{k,i} H_D (3 \cos^2\Theta_{r_{ik}z} - 1) \qquad /6/$$

Here "i" is the index of the given fluorine atom, "k" the index of the paramagnetic ion; r_{ik} is the distance between the k-th paramagnetic ion and the i-th fluorine atom; $\Theta_{r_{ik}z}$ is the angle between the external magnetic field and r_{ik}; H_D is the total dipole sum, its value being the same for each of the fluorine atoms. Summation for two neighbouring paramagnetic ions is sufficient.

Review of results reported in the literature

Shulman and Sugano [3] and Hirakawa [7,20] have measured the nucleus electron hyperfine interaction constants and spin densities for $KMnF_3$, $KCoF_3$, and $KNaCrF_6$ monocrystals. In evaluating their results we shall follow the approach of Hirakawa and Goodenough [14]. It should be noted that the spin densities arising at the fluorine atom give information about the delocalization of the unpaired 3d-electrons.

A_s, f_s

In the formation of the $\sigma^*(d(E_g))$ molecular orbital /see Fig.2/ $3d(E_g)$ - electrons admix with the 2s-electron orbitals of the fluorine atoms. By means of Fermi interaction these unpaired "magnetic" electrons produce an isotropic hyperfine field H_s at the site of the fluorine nucleus. In Mn^{2+} and Ni^{2+} ions the electron filling of the upper E_g symmetry level does not change, and thus there is no change in the spin density f_s either /Table III/. In $NaKCrF_6$ all the electrons are at the T_{2g} level and so the value of f_s is very small.

A_σ, f_σ

In the formation of the $\sigma^*(d(E_g))$ molecular orbital /Fig.2/ $3d(E_g)$-electrons are admixed with the $2p_\sigma(E_g)$-electron orbitals of the fluorine atoms. The unpaired electrons also produce a hyperfine field at the fluorine nucleus [8]. The behaviour of the nucleous-electron hyperfine interaction constant A_σ and the spin density f_σ is similar to that found for the 2s-electron orbital.

A_π, f_π

In the formation of the T_{2g}-symmetry $\pi^*(d(T_{2g}))$ molecular orbital /Fig. 2/ "magnetic" electrons are admixed with the $2p_\pi(T_{2g})$-electron orbitals of the fluorine atoms. The occupancy of this low-lying energy level increases in the series Mn^{2+}, Co^{2+}, Ni^{2+}, but the newer electrons enter the energy level in the opposite spin state. The decrease in the number of electrons with uncompensated spins causes a decrease in the negative A_π and f_π contributions. It is generally not possible to measure the A_σ and A_π nucleus-electron hyperfine interaction constants separately using NMR techniques, only their difference.

EXPERIMENTAL

Preparation of $KNiF_3$ and $RbFeF_3$

Polycrystalline samples of $KNiF_3$ were prepared from aqueous solution in a platinum vessel at 70°C, through the following reactions:

1/ $KHCO_3 + HF \longrightarrow KF + H_2O + CO_2$

2/ $3KF + NiCl_2 \longrightarrow KNiF_3 + 2KCl$

All chemicals were of analytical grade. The $KNiF_3$ precipitate was washed free of chloride and dried. The Ni content was determined by the dimethylglyoxime method.

After separation by the Willard-Winter method the fluorine content was determined by titration with thorium nitrate, using alizarin red indicator.

Observed Ni content : 37.8 ± 0.3 % Theoretical : 37.9 %

Observed F content : 36.5 ± 0.2 % Theoretical : 36.8 %

Polycrystalline samples of $RbFeF_3$ were obtained through the following reactions:

1/ $FeCl_2 + 2HF \longrightarrow FeF_2 + 2HCl$

2/ $RbF + FeF_2 \longrightarrow RbFeF_3$

Pure RbF and $FeCl_2$ and HF of analytical grade were used. The $RbF + FeF_2$ reaction was carried out in vacua in weldsealed platinum crucibles. Homogenized equimolecular amounts of the compounds were heated to 1050°C over 2 1/2 hours and then held at this temperature for 3 hours. The Fe^{3+} concentration in the $RbFeF_3$ was 1.2 ± 0.3 %, as measured by Mössbauer method. The fluorine content was determined in the same way as above for $KNiF_3$: a value of 29.3 ± 0.2 % was obtained, compared with the theoretical value of 28.7 %. The lattice constant for $RbFeF_3$ found by X-ray diffraction was $a = 4.167 \pm 0.005$ Å; the positions of the lines in the X-ray spectrum agreed with those reported by Kestigian [24].

NMR measurements

The values of the nucleus–electron hyperfine interaction constants A_σ and $A_{\sigma-\pi}$ and the spin densities f_s and $f_{\sigma\pi}$ were determined by NMR measurements in the paramagnetic state. The thermal average values $\langle s\rangle_{z,T}$ were calculated from literary data on susceptibility measurements.

A broad-line NMR spectrometer with a resolution of 10^{-5} was used for the measurements. An external field strength of 4500 G was employed. The signals were detected by the lock-in technique at a bandwidth of 0.01 c.p.s. and with a scanning time of 20 min per signal. By passing the weak-intensity NMR spectra through a 512-channel analyser operating in the collecting-and-averaging mode the signal-to-noise ratio was improved by an order of magnitude. The signal width was determined from signals obtained at 2.0 G amplitude field modulation, to avoid modulation distortion.

As powder samples were studied, the summation of the anisotropic contributions from the different orientations yielded a characteristic asymmetrical signal shape. The method of calculating this shape is given in the Appendix. The isotropic H_s and anisotropic H_D parameters can be determined from the signal shape after the dipole contribution has been deducted. The method of calculating the nculeus-electron hypefine interaction constants and the spin densities from these parameters is likewise given in the Appendix.

The NMR signals from polycrystalline $KNiF_3$ were taken in the temperature range 297 - 253°K. The signal shift, which is essentially determined by the isotropic H_s contribution, was measured from a teflon etalon. As expected, the coupling constant did not vary in the temperature range examined. The values of A_s and $A_{\sigma\pi}$ showed no temperature dependence of the susceptibility and the thermal average $\langle s\rangle_{z,T}$ in this temperature range. The susceptibility measurements of Hirakawa [20] were used in the calculations. Our values for the coupling constant and spin density agree with those obtained by Shulman and Sugano [3] on monocrystalline samples. The Néel point indicated by the strong drop in the intensity of the NMR signal was found to be 253 ± 5°K.

The measurements on plycrystalline $RbFeF_3$ were carried out in the temperature range 297 - 220°K. The hyperfine interactions and spin density showed no temperature dependence in this range. The sizes of the isotropic A_s and anisotropic $A_{\sigma\pi}$ parameters increased with decreasing temperature /Table II/, in accordance with the available susceptibility data /Wang and Kestigian [20]/.

Evaluation of the experimental results

1. $KNiF_3$

All NMR measurements reported in the literature for $KNiF_3$ are for monocrystalline samples only. Thus there seems to be a need for control measurements on a polycrystalline material with known properties, such as $KNiF_3$. The agreement between our data and those of Shulman and Sugano [3] shows that isotropic and anisotropic nucleus-electron hyperfine interaction constants can be determined from NMR investigations on polycrystalline materials too.

2. $RbFeF_3$

The spin densities of $RbMF_3$-type /M = paramagnetic ion/ perovskites corresponding to filling of the T_{2g} magnetic level should behave in the same way as the spin density in the KMF_3 series. However, the f_s spin density for $RbFeF_3$ is considerably reduced and $f_{\sigma-\pi}$ is, in fact, negative. The other members of the $RbMF_3$ series do not show this anomalous behaviour, and the hyperfine interaction constants and spin densities of the pairs $RbMnF_3$ - $KMnF_3$ and $RbNiF_3$ - $KNiF_3$ are close to one another /Table III/.

Since there is a high-spin state in $RbFeF_3$, the cause of this phanomenon cannot be attributed to electronic rearrangement [19]. It is possible, however, that the crystal structure is slightly deformed and that, contrary to assumption, states of other symmetries are formed.

APPENDIX

NMR spectra of monocrystals

The NMR spectra of AMF_3-type, perovskite-structure monocrystals /A = alkali metal; M = paramagnetic ion/ have two parts. The position of one of the parts is dependent on, that of the other part independent of, the orientation of the monocrystal in the external magnetic field. The positions of the two parts can be found from eqs. /1/ and /6/, and can be expressed as follows:

$$H_z = H^z_{deloc} + H^z_D = H_s + \sum_p H_{PD} (3 \cos\Theta_{pz} - 1) \qquad /7/$$

where H_z is the magnetic field at the site of the fluorine nucleus, "p" is the index for a fluorine atoms in non-equivalent lattice sites, H_s is the isotropic field contribution, and H_{PD} the anisotropic field constant.

In paramagnetic crystals the hyperfine interaction is dominant in forming the NMR spectrum, the other interactions cause merely a slight broadening of the signal. The broadened signal has the form of a Lorentzian curve [8].

The nucleus-electron hyperfine interaction constant A_s can be calculated from the isotropic contribution using expressions /1/ and /2/:

$$H_s = - \frac{\langle s \rangle_{z,T}}{\gamma\hbar} \cdot A_s \qquad /8/$$

The hyperfine interaction constant $A_{\sigma-\pi}$ for a given angle can be calculated from the anisotropic contribution of eqs. /1/ and /7/ after subtracting the dipole contribution eq. /6/ of the hyperfine interaction:

$$H_{PD} = \sum_{k=1}^{2} \frac{g\mu_B \langle s \rangle_{z,T}}{r_{ik}^{3}} + \frac{A_{\sigma-\pi}}{\gamma_N h} \langle s \rangle_{z,T} \qquad /9/$$

Susceptibility and the thermal average value of electrons with uncompensated spins

The thermal average of the electron spins of a paramagnetic ion can be determined from the magnetic susceptibility of the paramagnetic crystal using [16] the expression

$$\langle s \rangle_{z,\pi} = \chi_m . H_o / N g\mu_B \qquad /10/$$

Shape of NMR signals of a polycrystalline sample

The hyperfine interaction has two contributions, produced by the localized and delocalized electrons, respectively. These two contributions create an isotropic and an anisotropic field. In a polycrystalline sample the contributions, averaged and weighted over all possible directions, give a typical asymmetrical signal shape [10]. The averaging is carried out using formula /7/. If it is assumed that there is a 180^o super-exchange mechanism, then it is clear that the field at any "i"-index fluorine nucleus will be a function of the angle $\theta r_{ik} z$. The probability that a vector r_{ik} will form an angle θ with the external magnetic field can be shown to be proportional to a surface element $ds = 2\pi \sin\theta d\theta$ /see Fig. 3/.

The signal shape $f(H)$ is determined by the number of resonant nuclei (N) at a given field H :

$$f(H) = \frac{dN}{dH} \sim \frac{dS}{dH} = \frac{dS}{d\theta} \cdot \frac{d\theta}{dH} \qquad /11/$$

where H is given by

$$H = H_{PD} (3 \cos^2 - 1) \qquad /12/$$

Introducing the parameter $x = (H^z - H_s) / 3$, the function for the signal shape can be written

$$f(x) = \frac{1}{\sqrt{2x-1}} \qquad /13/$$

Taking into account the Lorentzian distribution of the individual signal shapes arising from the dipole-dipole and other effects building up the nucleus-electron interaction

$$f(x) = \frac{1}{\sqrt{3\pi}.\Delta x} \int_{-1/2}^{1} \frac{dg}{(1+2g)^{1/2}\left(1+ \frac{x-g}{(\Delta x)^2}\right)} \qquad /14/$$

where

$$\Delta x = \frac{\Delta H_L}{2H_{PD}} \quad , \quad x = \frac{H^z - H_s}{2H_{PD}}$$

As a consequence of the technique of detection it is the derivative of the NMR signal that is measured. After integration the shape of the derivative signal will be:

$$\frac{df(x)}{dx} = \frac{\Delta x}{\pi}\left\{\frac{1}{\sqrt{3}\cdot q}\left[\frac{-0.5q^2 + 2x + 1}{b}\,\ell n\,\frac{3 + 2\sqrt{3b} + q^2}{3 - \sqrt{3b} + q^2} + \right.\right.$$

$$\left.\left. + \frac{q^2 - 2(2x+1)}{a}\left(\mathrm{artg}\,\frac{\sqrt{3}+b}{a} + \mathrm{artg}\,\frac{\sqrt{3}-b}{a}\right)\right] + \frac{8(0.5 - 2x)}{q^4(q^4 - 12x + 3)}\right\} \qquad /15/$$

where

$$q^4 = 4(\Delta x)^2 + (2x+1)^2 \qquad a^2 = 0.5\,(q^2 - 2x - 1)$$

$$b^2 = 0.5\,(q^2 + 2x + 1)$$

The NMR signal of the paramagnetic powder sample was compared with the reference signal of a diamagnetic fluorine-containing material /teflon/ and the distance from the latter was measured /Fig. 4/. Denoting the individual signal width by ΔH_L, its value equals the width of the large signal measured at 0.7 of its height. Denoting the position of the large signal by C, point A is defined as lying a distance $(1/3)\Delta H_L$ from C. The distant local maximum is called D. The point where $H_s = H^z$ can be defined using the proportionality

$$AB : BD = 1 : 2$$

The error is very small if $\Delta x \ll 1$ [21]. H_s is equal to the distance EB, where E is the position of the signal of the diamagnetic material. H_{PD} is the distance AB. Knowing H_s and H_{PD} the nucleous-electron hyperfine interaction constants can be calculated using eqs. /8/ and /9/.

ACKNOWLEDGEMENTS

We would like to thank Dr. Kálmán Tompa for his guidance, for his support of our work, and for his useful comments. Further, we are grateful to Mrs. L. Zsoldos for carrying out the X-ray measurements, to I. Vincze for checking the Mössbauer measurements, and to A. Jánossy, Miss M. Hegyháti for their help over points of theory and measurement technique.

REFERENCES

[1] Al'tsuler Sz. A., Kozürev B.M.: Elektronnüj paramagnetnüj rezonansz /81. old./ Moszkva, 1961./

[2] Van Vleck J.H.: J. Chem. Phys., 3, 803 1935

[3] Shulman R.G., Sugano S.: Phys. Rev., 130, 506, 1963

[4] Turov E.A., Petrov M.T.: Jadernüj magnitnüj rezonansz v ferro i antiferromagnetikah. /Moszkva, 1969/.

[5] Matolcsy Erzsébet: Paramágneses molekulakristályok NMR vizsgálata. KFKI 1968. Diplomamunka.

[6] Simanek E., Sroubek Z.: Phys. Stat. Sol., 4, 251, 1964

[7] Hirakawa K.: J. Phys. Soc., Japan 19, 1678, 1964

[8] Abragam A.: The principles of nuclear magnetism. Oxford, 1961 /VI. fejezet, 6.§/.

[9] Slichter C.P.: Principles of Magnetic Resonance, New York, 1963

[10] Kroon D.J.: Philips Research Reports, 15, 501, 1960

[11] Hirakawa, K. Hashimoto T.: J. Phys. Soc. Japan, 15, 2063, 1960

[12] Stouth J.W., Shulman R,G.: Phys. Rev., 118, 1136, 1960

[13] Wang F., Kestigian M.: J. Appl. Phys., 37, 975, 1966

[14] Goodenough J.B.: Magnetism and the Chemical Bond, 1963, Interscience Publishers.

[15] Anderson P.W.: Sol. Stat. Phys., 14, 99, 1963

[16] Petrov M.P., Moszkalev B.B.: Fiz. Tverd. Tala, 12, 2063 1970

[17] Maarschall E.P.: Critical behaviour of the fluorine NMR linewidth in K_2MnF_4 and $KMnF_3$ above T. AMPÉRE Konferencia, Bukarest, 1970

[18] Szmolenszkij G.A., Petrov M.P., Moszkalev V.V., i dr.: Fiz. Tverd Tela, <u>10</u>, 1304, 1968

[19] Payne R.E., Forman R.A.: Proc. Phys. Soc., <u>84</u>, 410, 1964

[20] Hirakawa K.: J. Phys. Soc. Japan, <u>15</u>, 2063, 1960

[21] Moszkalev V.V.: Egyetemi előadás 1967. Leningrádi Állami Egyetem

[22] Walker M.B.: Proc. Phys. Soc., <u>87</u>, 45, 1966

[23] Elwell D.: J. Chem. Phys., <u>42</u>, 3806, 1965

[24] Kestigian M. et al.: Inorg. Chem., <u>5</u>, 1462, 1966

Table 1

Measured data for $KNiF_3$

$T[K^o]$	$\chi \cdot 10^{-3}$ $[mol^{-1}]$	$\langle s \rangle_{z,T} \cdot 10^{-4}$	$H_s[G]$	$A_s[cm^{-1}] \cdot 10^{-4}$	$f_s[\%]$	$H_{PD}[G]$	H_D	$A_\sigma - A_\pi [cm^{-1}] \cdot 10^{-4}$	$f_{\sigma-\pi}[\%]$
297	2.0±0.1	6.9±0.3	26.7±0.4	32±4	0.50±0.05	11,2±0.2	3.8	9.0±1.5	3.5±0.5
283	2.0±0.1	6.9±0.3	25.6±0.4	32±4	0.50±0.05	10.8±0.2	3.8	o.01±1.5	3.5±0.5
273	2.0±o;1	6.9±0.3	25.2±0.4	31±4	0.48±0.05	10.0±0.2	3.8	8.2±1.5	3.2±0.5
263	2.0±0.1	6.9±0.3	23.9±0.4	30±4	0.45±0.05	9.8±0.2	3.8	8.0±1.5	3.1±0.5

Table II

Measured data for $RbFeF_3$

$T[K^o]$	$\chi.10^{-3}$ mol^{-1}	$<s>_{z,T}\cdot10^{-3}$	$H_s[G]$	$A_s[cm^{-1}]\cdot10^{-4}$	$f_s\|\%\|$	$H_{PD}[G]$	$H_D[G]$	$A_\sigma-A_\pi cm^{-1}\cdot10^{-4}$	$f_{\sigma-\pi}[\%]$
297	8.3	5.5±0.2	33.2±0.5	8.5±1.0	0.22±0.04	6.4±0.5	11.8±5	-0.3±0.2	-0.27±0.2
275	8.9	6.9±0.2	35.7±0.5	8.5±1.0	0.22±0.04	7.5±0.5	13±5	-0.3±0.2	-0.27±0.2
240	10.2	7.0±0.2	40.2±0.8	8.5±1.0	0.22±0.04	9.7±0.8	15±5	-0.3±0.2	-0.27±0.2
223	10.7	7.5±0.2	42.5±1.0	8.5±1.0	0.22±0.04	11.7±0.8	16±5	-0.3±0.2	-0.27±0.2

Table III

Our own and literary data for the KMF_3 and $RbMF_3$ series /M = Mn,Ni,Co,Fe/

Compound	3d-elect. structure. in octahedral field		F-M distance Å	exchange constant J	$A_s \cdot 10^{-4}$ $[cm^{-1}]$	f_s [%]	$A_\sigma - A_\pi \cdot 10^{-4}$ $[cm^{-1}]$	$f_{\sigma-\pi}$ [%]	Crystal structure	Magnetic below T_N
	T_{2g}	E_g								
$KMnF_3$	↑↑↑	↑↑	2.093	8.9	16.26	0.52	0.17	0.17	C_{2h}^2	G
$KCoF_3$	↑↓↑↓	↑↑	2.03	11.19	25	0.55	8.2	5.7	C_{2h}^2	G
$KNiF_3$	↑↓↑↓↑	↑↑	2.06	45	33.9	0.50	10.9	+4.90	C_{2h}^2	G
$KNaCrF_6$	↑↑↑				- 1.1	-0.02	-7.2	-4.95		
$RbMnF_3$	↑↑↑	↑↑	2.11	3.3	15.68	0.50	0.31	0.33	C_{2h}^2	G
$RbFeF_3$	↑↓↑↑	↑↑	2.08	43.9	8.5±1.0	0.22±0.04	-0.3±0.2	-0.27±0.2	C_{2h}^2	weakly ferromagnetic 101°K<T<87°K
$RbNiF_3$	↑↓↑↓↑↓	↑↑		36	41 34	0.5 0.45	12	5.6	D_{6h}^4	two non-equivalent sublattices, ferromagnetic

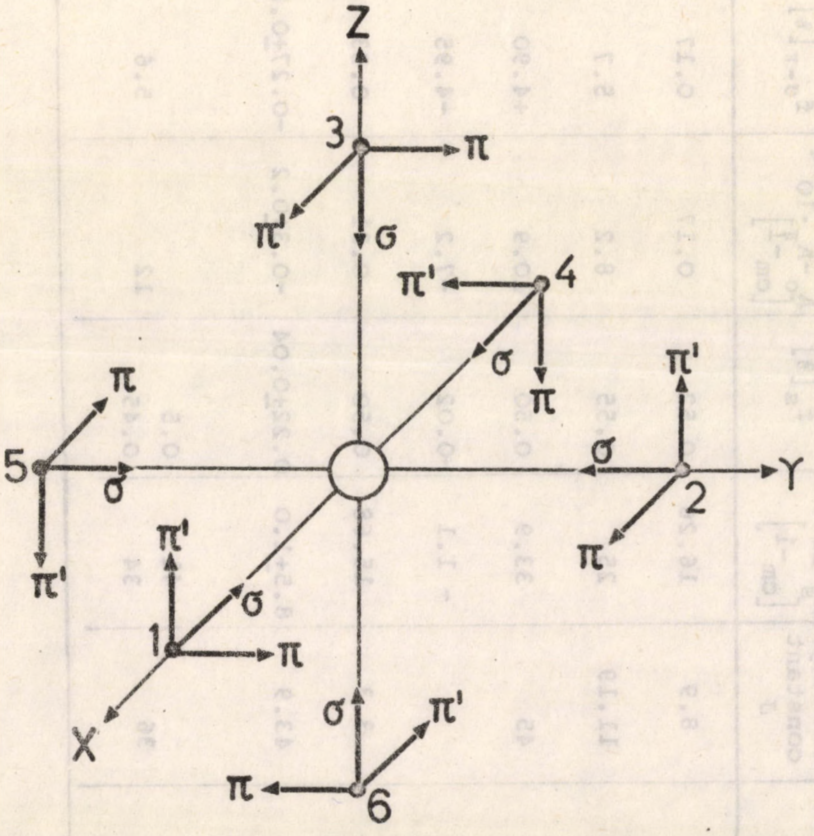

Fig. 1

Position of the electron orbitals in MX_6-type complexes in a crystal field of octahedral symmetry. The fluorine atoms are numbered 1, 2, ..., 6

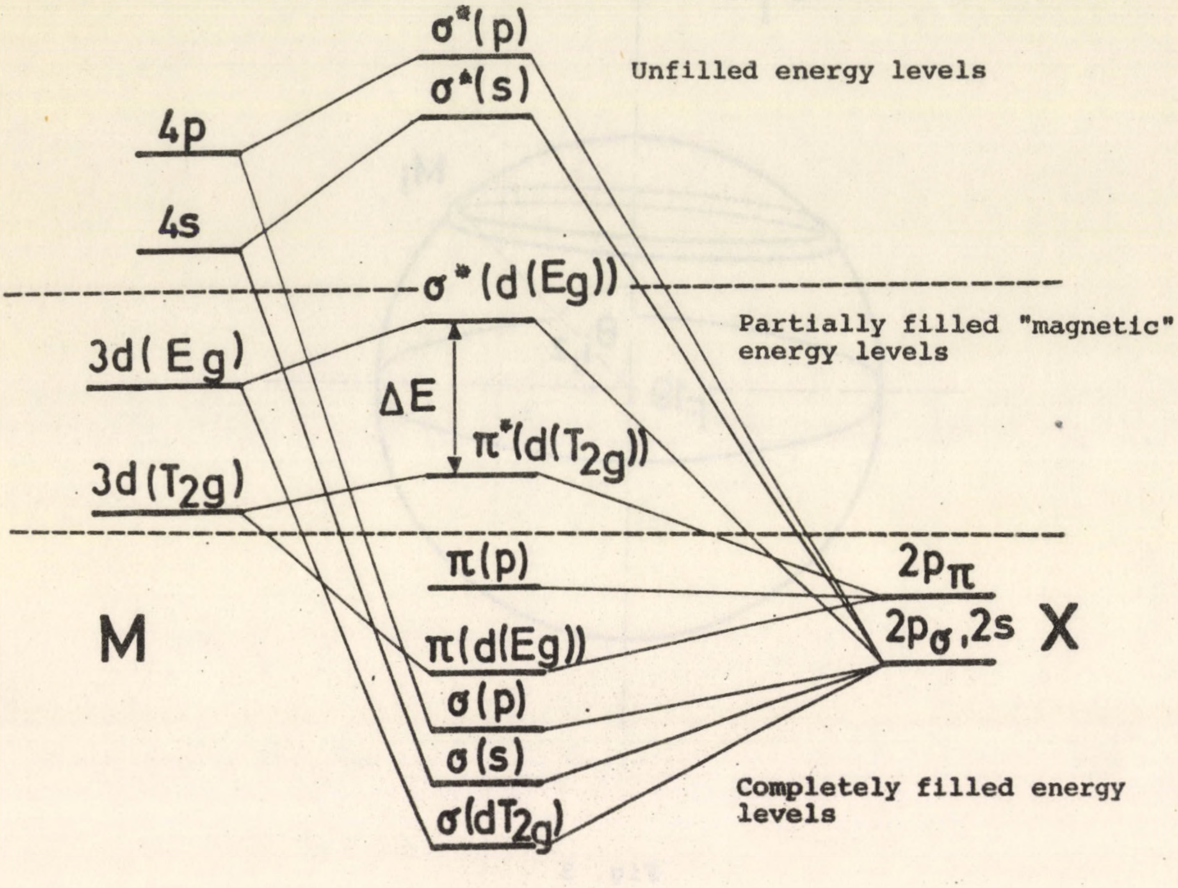

Fig. 2

Energy levels of molecular orbitals in MX_6-type complexes. T_{2g} and E_g symmetries in an octahedral field.

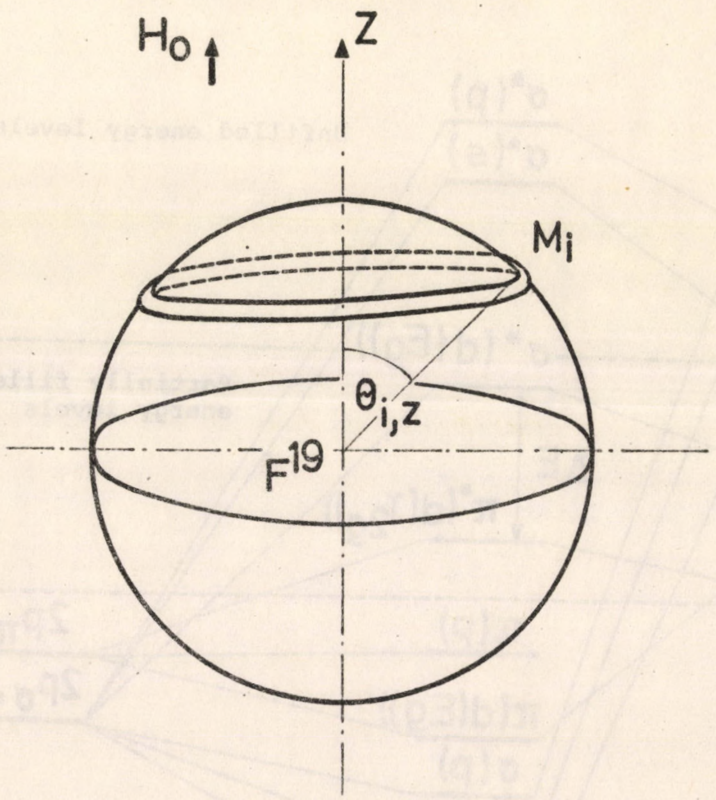

Fig. 3

Model used in the calculation of the shape of NMR signals from powder samples. The paramagnetic ions /M_i/ are uniformly distributed over the surface of the sphere.

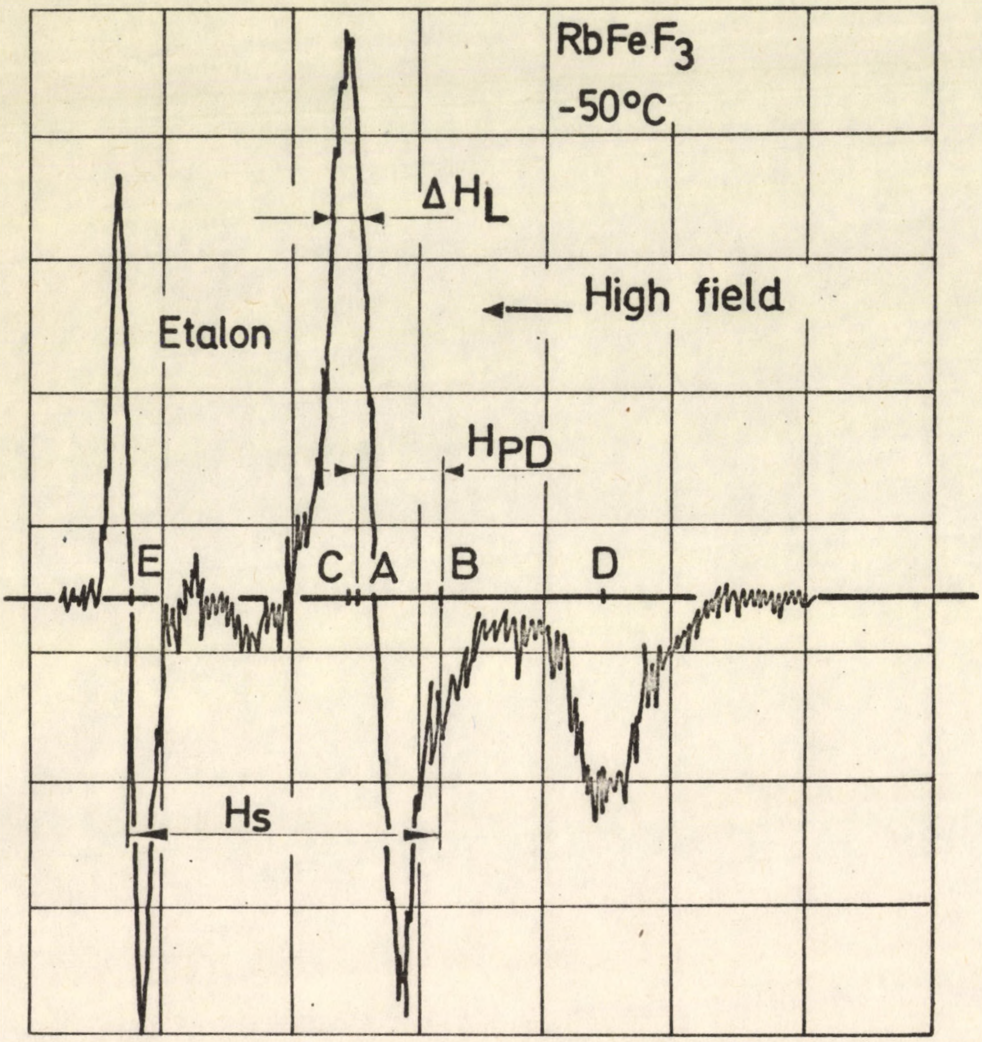

Fig. 4

Shape of NMR signal from $RbFeF_3$ powder sample H_s is the isotropic distortion, P_{PD} is the anisotropic constant. The explanation of the other signs can be found in the Appendix

Kiadja a Központi Fizikai Kutató Intézet
Felelős kiadó: Tompa Kálmán, a KFKI
Szilárdtestfizika Tudományos Tanácsának
elnöke
Szakmai lektor: Hegyháti Magdolna
Nyelvi lektor: T. Wilkinson
Példányszám: 255   Törzsszám: 71-5922
Készült a KFKI sokszorositó üzemében, Budapest
1971. szeptember hó